

Seesaw-type and low-scale models of neutrino masses are reviewed, along with the corresponding structure of the lepton mixing matrix. The status of neutrino oscillation parameters as of June 2006 is given, including recent fluxes, as well as latest SNO, K2K and MINOS results. Some prospects for the next generation of experiments are given. This writeup updates the material presented in my lectures at the Corfu Summer Institute on Elementary Particle Physics in September 2005.

# Contents

<b>1</b>	<b>Introduction</b>	<b>2</b>
<b>2</b>	<b>Dirac and Majorana masses</b>	<b>3</b>
<b>3</b>	<b>The origin of neutrino mass</b>	<b>7</b>
3.1	Seesaw and related models . . . . .	8
3.1.1	“Effective” seesaw . . . . .	9
3.1.2	The “1-2-3” seesaw mechanism . . . . .	10
3.1.3	Left-right symmetric and $SO(10)$ . . . . .	11
3.1.4	“Double” seesaw mechanism . . . . .	12
3.1.5	“Novel” $SO(10)$ seesaw mechanism . . . . .	13
3.2	Low-scale models . . . . .	14
3.2.1	Radiative models . . . . .	15
3.2.2	Supersymmetry and neutrino mass . . . . .	15
3.2.3	“Inverse” seesaw mechanism . . . . .	16
<b>4</b>	<b>The lepton mixing matrix</b>	<b>17</b>
4.1	Dirac case . . . . .	17
4.2	Majorana case . . . . .	19
4.3	Seesaw-type mixing . . . . .	20

<b>5</b>	<b>Phenomenology</b>	<b>22</b>
5.1	Status of neutrino oscillations . . . . .	22
5.2	Predicting neutrino masses and mixing . . . . .	25
5.3	Absolute scale of neutrino mass and $0\nu\beta\beta$ . . . . .	26
5.4	Other phenomena . . . . .	27
5.4.1	Majoron physics . . . . .	28
5.4.2	New gauge boson . . . . .	29
5.4.3	Lepton flavour violation . . . . .	29
5.4.4	Reconstructing neutrino mixing at accelerators . . . . .	31
5.5	Thermal leptogenesis . . . . .	32
<b>6</b>	<b>Non-standard neutrino interactions</b>	<b>33</b>
6.1	Atmospheric neutrinos . . . . .	34
6.2	Solar neutrinos . . . . .	34

# 1 Introduction

The historic discovery of neutrino oscillations [1–5] marks a turning point in particle and nuclear physics and implies that neutrinos have mass. This possibility has been first suggested by theory since the early eighties, both on general grounds and on the basis of different versions of the seesaw mechanism [6–11].

The general characterization of neutrino mass theories in  $SU(3) \otimes SU(2) \otimes U(1)$  terms provided a model-independent basis to analyse the seesaw [9,10]. It also indicated a fundamental difference between the lepton and the quark mixing matrices, namely, the appearance of new phases associated to the Majorana nature of neutrinos [9].

Irrespective of what the ultimate origin of neutrino mass may turn out to be, the basic gauge theoretic mechanism to account for the smallness of neutrino mass is in terms of the feebleness of B-L violation. The seesaw is one realization of the idea, by far not unique. There are two classes of theories of neutrino mass, that differ by the scale at which L-symmetry is broken. They are summarized in Sec. 3. The corresponding structure of the lepton mixing matrix that follows from theory is described Sec. 4. This forms the basis for the analysis of the data from current neutrino oscillation experiments [1–5] [12,13]. The status of neutrino mass and mixing parameters as determined from the world’s neutrino oscillation data within the simplest CP-conserving three-neutrino mixing scheme is summarized in Sec. 5.1 [14]. In addition a determination of

the solar angle  $\theta_{12}$ , the atmospheric angle  $\theta_{23}$  and the corresponding mass squared splittings  $\Delta m_{\text{SOL}}^2$  and  $\Delta m_{\text{ATM}}^2$ , one gets a constraint on the last angle in the three–neutrino leptonic mixing matrix,  $\theta_{13}$ . Together with the small ratio  $\Delta m_{\text{SOL}}^2/\Delta m_{\text{ATM}}^2$  the angle  $\theta_{13}$  holds the key for further progress in neutrino oscillation searches.

Some attempts at predicting neutrino masses and mixing are given in Sec. 5.2. Lepton number violating processes such as neutrinoless double beta decay [15,16] are briefly discussed in Sec. 5.3. Searching for  $0\nu\beta\beta$  constitutes a very important goal for the future, as this will probe the fundamental nature of neutrinos, irrespective of the process that induces it, a statement known as the “black-box” theorem [17]. In addition,  $0\nu\beta\beta$  will be sensitive to the absolute scale of neutrino mass and to CP violation induced by the so-called Majorana phases [9], inaccessible in conventional oscillations [18–20]. Finally in Sec. 6 the robustness of the oscillation interpretation and the role of non-standard neutrino interactions in future precision oscillation studies is briefly mentioned.

## 2 Dirac and Majorana masses

Electrically charged fermions must be Dirac type. In contrast, electrically neutral fermions, like neutrinos (or supersymmetric “inos”), are expected to be Majorana-type on general grounds, irrespective of how they acquire their mass. Phenomenological differences between Dirac and Majorana neutrinos are tiny for most processes, such as neutrino oscillations: first because neutrinos are known to be light and, second, because the weak interaction is chiral, well described by the V-A form.

The most basic spin 1/2 fermion corresponding to the lowest representation of the Lorentz group is given in terms of a 2-component spinor  $\rho$ , with the following free Lagrangean [9]

$$\mathcal{L}_M = -i\rho^\dagger\sigma_\mu\partial_\mu\rho - \frac{m}{2}\rho^T\sigma_2\rho + H.C. \quad (1)$$

where  $\sigma_i$  are the usual Pauli matrices and  $\sigma_4 = -iI$ ,  $I$  being the  $2 \times 2$  identity matrix. I use Pauli’s metric conventions, where  $a.b \equiv a_\mu b_\mu \equiv \vec{a} \cdot \vec{b} + a_4 b_4$ ,  $a_4 = ia_0$ . Under a Lorentz transformation,  $x \rightarrow \Lambda x$ , the spinor  $\rho$  transforms as  $\rho \rightarrow S(\Lambda)\rho(\Lambda^{-1}x)$  where  $S$  obeys

$$S^\dagger\sigma_\mu S = \Lambda_{\mu\nu}\sigma_\nu \quad (2)$$

The kinetic term in Eq. (1) is clearly invariant, and so is the mass term, as a result of unimodular property  $\det S = 1$ . However, the mass term is not invariant under a

phase transformation

$$\rho \rightarrow e^{i\alpha} \rho \quad (3)$$

The equation of motion following from Eq. (1) is

$$-i\sigma_\mu \partial_\mu \rho = m\sigma_2 \rho^* \quad (4)$$

As a result of the conjugation and Clifford properties of the  $\sigma$ -matrices, one can verify that each component of the spinor  $\rho$  obeys the Klein-Gordon wave-equation.

Start from the usual Lagrangean describing of a massive spin 1/2 Dirac fermion, given as

$$\mathcal{L}_D = -\bar{\Psi} \gamma_\mu \partial_\mu \Psi - m \bar{\Psi} \Psi, \quad (5)$$

where by convenience we use the chiral representation of the Dirac algebra  $\gamma_\mu \gamma_\nu + \gamma_\nu \gamma_\mu = 2 \delta_{\mu\nu}$  in which  $\gamma_5$  is diagonal,

$$\gamma_i = \begin{pmatrix} 0 & -i\sigma_i \\ i\sigma_i & 0 \end{pmatrix} \quad \gamma_4 = \begin{pmatrix} 0 & I \\ I & 0 \end{pmatrix} \quad \gamma_5 = \begin{pmatrix} I & 0 \\ 0 & -I \end{pmatrix}. \quad (6)$$

In this representation the charge conjugation matrix  $C$  obeying

$$C^T = -C \quad (7)$$

$$C^\dagger = C^{-1} \quad (8)$$

$$C^{-1} \gamma_\mu C = -\gamma_\mu^T \quad (9)$$

is simply given in terms of the basic conjugation matrix  $\sigma_2$  as

$$C = \begin{pmatrix} -\sigma_2 & 0 \\ 0 & \sigma_2 \end{pmatrix}. \quad (10)$$

In order to display clearly the relationship between the Majorana theory in Eq. (1) and the familiar Dirac Lagrangean in Eq. (5), one splits a Dirac spinor as

$$\Psi_D = \begin{pmatrix} \chi \\ \sigma_2 \phi^* \end{pmatrix}, \quad (11)$$

so that the corresponding charge-conjugate spinor  $\Psi_D^c = C \bar{\Psi}_D^T$  is the same as  $\Psi_D$  but exchanging  $\phi$  and  $\chi$ , i. e.

$$\Psi_D^c = \begin{pmatrix} \phi \\ \sigma_2 \chi^* \end{pmatrix}. \quad (12)$$

A 4-component spinor is said to be Majorana or self-conjugate if  $\Psi = C\bar{\Psi}^T$  which amounts to setting  $\chi = \phi$ . Using Eq. (11) we can rewrite Eq. (5) as

$$\mathcal{L}_D = -i \sum_{\alpha=1}^2 \rho_{\alpha}^{\dagger} \sigma_{\mu} \partial_{\mu} \rho_{\alpha} - \frac{m}{2} \sum_{\alpha=1}^2 \rho_{\alpha}^T \sigma_2 \rho_{\alpha} + H.C. \quad (13)$$

where

$$\begin{aligned} \chi &= \frac{1}{\sqrt{2}}(\rho_2 + i\rho_1) \\ \phi &= \frac{1}{\sqrt{2}}(\rho_2 - i\rho_1) \end{aligned} \quad (14)$$

are the left handed components of  $\Psi_D$  and of the charge-conjugate field  $\Psi_D^c$ , respectively. This way the Dirac fermion is shown to be equivalent to two Majorana fermions of equal mass. The  $U(1)$  symmetry of the theory described by Eq. (5) under  $\Psi_D \rightarrow e^{i\alpha}\Psi_D$  corresponds to continuous rotation symmetry between  $\rho_1$  and  $\rho_2$

$$\begin{aligned} \rho_1 &\rightarrow \cos \theta \rho_1 + \sin \theta \rho_2 \\ \rho_2 &\rightarrow -\sin \theta \rho_1 + \cos \theta \rho_2 \end{aligned}$$

which result from the mass degeneracy between the  $\rho$ 's, showing that, indeed, the concept of fermion number is not basic.

The mass term in Eq. (1) vanishes unless  $\rho$  and  $\rho^*$  are anti-commuting, so the Majorana fermion is, right from the start, a quantized field. The solutions to Eq. (1) are easily obtained in terms of those of Eq. (5), which are well known:

$$\Psi_M = (2\pi)^{-3/2} \int d^3k \sum_{r=1}^2 \left(\frac{m}{E}\right)^{1/2} [e^{ik \cdot x} A_r(k) u_{Lr}(k) + e^{-ik \cdot x} A_r^{\dagger}(k) v_{Lr}(k)], \quad (15)$$

where  $u = C\bar{v}^T$  and  $E(k) = (\vec{k}^2 + m^2)^{1/2}$  is the mass-shell condition. The creation and annihilation operators obey canonical anti-commutation rules and, like the  $u$ 's and  $v$ 's, depend on the momentum  $k$  and helicity label  $r$ . The expression in Eq. (15) describes the basic Fourier expansion of a massive Majorana fermion. It differs from the usual Fourier expansion for the Dirac spinor in Eq. (16) in two ways:

- spinors are two-component, as there is a chiral projection on the  $u$ 's and  $v$ 's
- there is only one Fock space, particle and anti-particle coincide, showing that a massive Majorana fermion corresponds to one half of a conventional massive Dirac fermion.

The  $u$ 's and  $v$ 's are the same wave functions that appear in the Fourier decomposition the Dirac field

$$\Psi_D = (2\pi)^{-3/2} \int d^3k \sum_{r=1}^2 \left(\frac{m}{E}\right)^{1/2} [e^{ik \cdot x} a_r(k) u_r(k) + e^{-ik \cdot x} b_r^\dagger(k) v_r(k)] . \quad (16)$$

Using the helicity eigenstate wave-functions,

$$\vec{\sigma} \cdot \vec{k} u_L^\pm(k) = \pm |\vec{k}| u_L^\pm(k) \quad (17)$$

$$\vec{\sigma} \cdot \vec{k} v_L^\pm(k) = \mp |\vec{k}| v_L^\pm(k) \quad (18)$$

one can show that, out of the 4 linearly independent wave functions  $u_L^\pm(k)$  and  $v_L^\pm(k)$ , only two survive as the mass approaches zero, namely,  $u_L^-(k)$  and  $v_L^+(k)$  [21]. This way the Lee-Yang two-component massless neutrino theory is recovered as the massless limit of the Majorana theory.

Two independent propagators follow from Eq. (1),

$$\langle 0 | \rho(x) \rho^*(y) | 0 \rangle = i \sigma_\mu \partial_\mu \Delta_F(x - y; m) \quad (19)$$

$$\langle 0 | \rho(x) \rho(y) | 0 \rangle = m \sigma_2 \Delta_F(x - y; m) \quad (20)$$

where  $\Delta_F(x - y; m)$  is the usual Feynman function. The first one is the “normal” propagator that intervenes in total lepton number conserving ( $\Delta L = 0$ ) processes, while the one in Eq. (20) describes the virtual propagation of Majorana neutrinos in  $\Delta L = 2$  processes such as neutrinoless double-beta decay.

The Lagrangean in Eq. (1) can easily be generalized to an arbitrary number of Majorana neutrinos, giving

$$L_M = -i \sum_{\alpha=1}^n \rho_\alpha^\dagger \sigma_\mu \partial_\mu \rho_\alpha - \frac{1}{2} \sum_{\alpha, \beta=1}^n M_{\alpha\beta} \rho_\alpha^T \sigma_2 \rho_\beta + H.C. \quad (21)$$

where the sum runs over the “neutrino-type” indices  $\alpha$  and  $\beta$ . By Fermi statistics the mass coefficients  $M_{\alpha\beta}$  must form a symmetric matrix, in general complex. This matrix can always be diagonalized by a complex  $n \times n$  unitary matrix  $U$  (See [9] for the proof)

$$M_{diag} = U^T M U . \quad (22)$$

When  $M$  is real its diagonalizing matrix  $U$  may be chosen to be orthogonal and, in general, the mass eigenvalues can have different signs. These may be assembled as a signature matrix

$$\eta = diag(+, +, \dots, -, -, \dots) \quad (23)$$

	$SU(3) \otimes SU(2) \otimes U(1)$
$L_a = (\nu_a, l_a)^T$	$(1, 2, -1)$
$e_a^c$	$(1, 1, 2)$
$Q_a = (u_a, d_a)^T$	$(3, 2, 1/3)$
$u_a^c$	$(\bar{3}, 1, -4/3)$
$d_a^c$	$(\bar{3}, 1, 2/3)$
$\Phi$	$(1, 2, 1)$

Table 1: Matter and scalar multiplets of the Standard Model (SM)

For two neutrino types there are two classes of models, one with  $\eta = \text{diag}(+, -)$  and another characterized by  $\eta = \text{diag}(+, +)$ . The class with  $\eta = \text{diag}(+, -)$  contains as a limit the case where the two fermions make up a Dirac neutrino. Note that one can always make all masses positive by introducing appropriate phase factors in the wave functions, such as the factors of  $i$  in Eq. (14). However, when interactions are added these signs become physical. As emphasized by Wolfenstein, they play an important role in the discussion of  $0\nu\beta\beta$  (neutrinoless double beta decay) [22].

### 3 The origin of neutrino mass

Table 1 gives the fifteen basic building blocks of matter. They are all 2-component sequential “left-handed” chiral fermions, one set for each generation. Parity violation in the weak interaction is incorporated “effectively” by having “left” and “right” fermions transform differently with respect to the  $SU(3) \otimes SU(2) \otimes U(1)$  gauge group. In contrast to charged fermions, neutrinos come only in one chiral species.

It has been long noted by Weinberg [8] that one can add to the Standard  $SU(3) \otimes SU(2) \otimes U(1)$  Model (SM) an effective dimension-five operator  $\mathcal{O} = \lambda L\Phi L\Phi$  where  $L$  denotes a lepton doublet for each generation and  $\Phi$  is the SM scalar doublet.

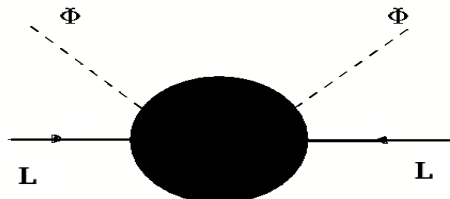


Figure 1: Dimension five operator responsible for neutrino mass [8].

Once the electroweak symmetry breaks through the nonzero vacuum expectation value (vev)  $\langle\Phi\rangle$ , Majorana neutrino masses  $\propto\langle\Phi\rangle^2$  are induced, in contrast to the masses of the charged fermions which arise from basic renormalizable interactions, and are linear in  $\langle\Phi\rangle$ . Moreover, the dimension-five operator  $\mathcal{O}$  violates lepton number by two units ( $\Delta L = 2$ ), whereas the charged fermion masses arise from renormalizable L-conserving Yukawa interactions. This naturally accounts for the smallness of neutrino masses irrespective of the specific origin of neutrino mass. From such general point of view the emergence of Dirac neutrinos would be a surprise, justified only in the presence of an “accidental” lepton number symmetry. For example, neutrinos could naturally get very small Dirac masses via mixing with a bulk fermion in models involving extra dimensions [23–25]. Barring such very special circumstances, gauge theories give rise to Majorana neutrinos.

Little more can be said from first principles about the *mechanism* giving rise to the operator in Fig. 1, its associated mass *scale* or its *flavour structure*. For example, the strength  $\lambda$  of the operator  $\mathcal{O}$  may be suppressed by a large scale  $M_X$  in the denominator (top-down) scenario, leading to

$$m_\nu = \lambda_0 \frac{\langle\Phi\rangle^2}{M_X},$$

where  $\lambda_0$  is some unknown dimensionless constant. Gravity, which in a sense “belongs” to the SM, could induce the dimension-five operator  $\mathcal{O}$ , providing the first example of a top-down scenario with  $M_X = M_P$ , the Planck scale [26]. In this case the magnitude of the resulting Majorana neutrino masses are too small.

Alternatively, the strength  $\lambda$  of the operator  $\mathcal{O}$  may be suppressed by small parameters (e.g. scales, Yukawa couplings) in the numerator and/or loop-factors (bottom-up scenario). Both classes of scenarios are viable and have many natural realizations. While models of the top-down type are closer to the idea of unification, bottom-up schemes are closer to experimental test.

Models of neutrino mass may also be classified according to whether or not additional neutral heavy states are present, in addition to the three isodoublet neutrinos. As an example, such leptons could be  $SU(3) \otimes SU(2) \otimes U(1)$  singlet “right-handed” neutrinos. In what follows we first consider top-down, then bottom-up scenarios.

### 3.1 Seesaw and related models

The most popular top-down scenario is the seesaw [6]. The idea is to generate the operator  $\mathcal{O}$  by the exchange of heavy states, both fermions (type-I) and scalars (type-II), as

shown in Fig. 2. This can be implemented in many ways, with different gauge groups

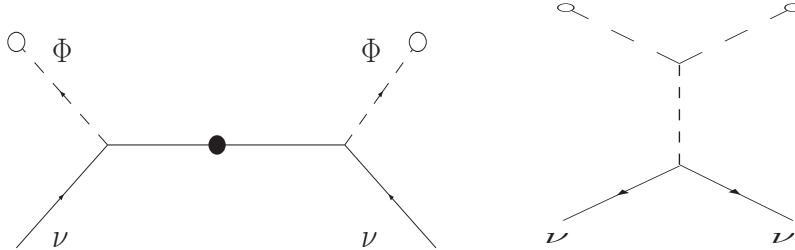


Figure 2: Two types of seesaw mechanism [6–11]

and multiplet contents. The main point is that, as the masses of the intermediate states go to infinity, neutrinos naturally become light [7]. The seesaw provides a simple realization of Weinberg’s operator [8]. Note that the seesaw idea does not require the gauging of B-L, nor does it require it to be broken spontaneously. In fact, most of the physics it encodes, and which has been brilliantly confirmed by the recent oscillation experiments, lies in its “effective” low-energy form [9]. Only in low-scale schemes like the inverse-seesaw discussed in Sec. 3.2.3 effects associated with “seesaw-dynamics” may be observable (see Secs. 5.4.1 and 5.4.2).

### 3.1.1 “Effective” seesaw

Much of the low energy phenomenology, such as that of neutrino oscillations is blind to the details of the underlying seesaw theory at high energies, e. g. its gauge group, multiplet content or the nature of B-L. For this purpose the most general way to describe the physics of the seesaw is to characterize it, effectively, in terms of the SM gauge structure [9]. In the basis  $\nu_L, \nu_L^c$ , corresponding to the three “left” and three “right” neutrinos, respectively, the seesaw mass matrix has SU(2) triplet, doublet and singlet terms described as [9]

$$\mathcal{M}_\nu = \begin{pmatrix} M_1 & D \\ D^T & M_2 \end{pmatrix}. \quad (24)$$

Here we use the original notation of reference [9], where the “Dirac” entry is proportional to  $\langle \Phi \rangle$ , the  $M_1$  comes from a triplet vev, and  $M_2$  may be added by hand, as it is a gauge singlet. The particular case  $M_1 = 0$  was first mentioned in Ref. [6].

Note that, though symmetric, by the Pauli principle, the matrix  $\mathcal{M}_\nu$  is complex, so that its Yukawa coupling sub-matrices  $D$  as well as  $M_1$  and  $M_2$  are also complex matrices, the last two symmetric. It is diagonalized by performing a unitary transformation

$U_\nu$ ,

$$\nu_i = \sum_{a=1}^6 (U_\nu)_{ia} n_a, \quad (25)$$

so that

$$U_\nu^T \mathcal{M}_\nu U_\nu = \text{diag}(m_i, M_i). \quad (26)$$

This yields 6 mass eigenstates, including the three light neutrinos with masses  $m_i$ , and three two-component heavy leptons of masses  $M_i$ . The light neutrino mass states  $\nu_i$  are given in terms of the flavour eigenstates via eq. (25). The effective light neutrino mass, obtained this way is of the form

$$m_\nu \simeq M_1 - DM_2^{-1}D^T. \quad (27)$$

The smallness of light neutrino masses is understood by assuming  $M_2 \gg D \gg M_1$ . The above general structure forms the basis for the description of the seesaw lepton mixing matrix [9], given in Sec. 4.3.

While it constitutes the most general description, and also the common denominator of all seesaw schemes, such an “effective” seesaw does not give a dynamical insight on the origin of neutrino mass. For this reason we now turn to schemes where lepton number symmetry is broken spontaneously.

### 3.1.2 The “1-2-3” seesaw mechanism

The simplest possibility for the seesaw is to have ungauged lepton number. It is also the most general, as it can be studied in the framework of just the  $SU(3) \otimes SU(2) \otimes U(1)$  gauge group. The mass terms in eq. (24) are given by triplet, doublet and singlet vevs, respectively, as [10]

$$\mathcal{M}_\nu = \begin{pmatrix} Y_3 v_3 & Y_\nu \langle \Phi \rangle \\ Y_\nu^T \langle \Phi \rangle & Y_1 v_1 \end{pmatrix} \quad (28)$$

As already mentioned, the Yukawa coupling sub-matrices  $Y_\nu$  as well as  $Y_3$  and  $Y_1$  are complex matrices, the last two symmetric.

The new dynamical insight provided by such “1-2-3” seesaw containing singlet, doublet and triplet scalar multiplets, is that they obey a simple vev seesaw relation of the type

$$v_3 v_1 \sim v_2^2 \quad \text{with} \quad v_1 \gg v_2 \gg v_3 \quad (29)$$

where  $v_2 \equiv \langle \Phi \rangle$  denotes the SM Higgs doublet vev, fixed by the W-boson mass. This hierarchy implies that the triplet vev  $v_3 \rightarrow 0$  as the singlet vev  $v_1$  grows. This is

consistent with the minimization of the corresponding  $SU(3) \otimes SU(2) \otimes U(1)$  invariant scalar potential, and implies that the triplet vev is “induced”.

Small neutrino masses arise either by heavy  $SU(3) \otimes SU(2) \otimes U(1)$  singlet “right-handed” neutrino exchange (type I) or by the small effective triplet vev (type II), as illustrated in Fig. 2. The effective light neutrino mass becomes,

$$m_\nu \simeq Y_3 v_3 - Y_\nu Y_1^{-1} Y_\nu^T \frac{\langle \Phi \rangle^2}{v_1} \quad (30)$$

The corresponding seesaw diagonalization matrices can be given explicitly as a systematic matrix perturbation series expansion in  $DM_2^{-1}$ , given in Ref. [10].

In such “1-2-3” seesaw, since lepton number is ungauged, there is a physical Goldstone boson associated with its spontaneous breakdown, the majoron [27]. Its profile can be determined on symmetry grounds and its couplings to neutrinos can be found systematically, see [10] for details.

### 3.1.3 Left-right symmetric and $SO(10)$

A more symmetric setting for the seesaw is a gauge theory containing B-L as a generator, such as  $SU(3) \otimes SU(2)_L \otimes SU(2)_R \otimes U(1)_{B-L}$  or the unified models based on  $SO(10)$  or  $E(6)$  [6, 7, 11]. For example in  $SO(10)$  each matter generation is naturally assigned to a **16** (spinorial in  $SO(10)$ ) so that the **16** . **16** . **10** and **16** . **126** . **16** couplings generate all entries of the seesaw neutrino mass matrix,

$$\mathcal{M}_\nu = \begin{pmatrix} Y_L \langle \Delta_L \rangle & Y_\nu \langle \Phi \rangle \\ Y_\nu^T \langle \Phi \rangle & Y_R \langle \Delta_R \rangle \end{pmatrix}. \quad (31)$$

Here the basis is  $\nu_L, \nu_L^c$ , as before,  $Y_L$  and  $Y_R$  denote the Yukawas of the **126** of  $SO(10)$ , whose vevs  $\langle \Delta_{L,R} \rangle$  give rise to the Majorana terms. They correspond to  $Y_1$  and  $Y_3$  of the simplest “1-2-3” model. On the other hand  $Y_\nu$  denotes the **16** . **16** . **10** Dirac Yukawa coupling. In  $SO(10)$  one has a discrete parity symmetry which implies  $Y_L = Y_R$  and  $Y_\nu = Y_\nu^T$  as recently emphasized in Ref. [28]. Since this may get broken, we prefer to keep, for generality,  $Y_L, Y_R$  as independent.

Small neutrino masses are induced either by heavy  $SU(3) \otimes SU(2) \otimes U(1)$  singlet “right-handed” neutrino exchange (type I) or heavy scalar boson exchange (type II) as illustrated in Fig. 2. The matrix  $\mathcal{M}_\nu$  is diagonalized by a unitary mixing matrix  $U_\nu$  as before. The diagonalization matrices can be worked out explicitly as a perturbation series, using the same method of Ref. [10]. This means that the explicit formulas for the  $6 \times 6$  unitary diagonalizing matrix  $U$  given in Ref. [10] also hold in the left-right case, provided one takes into account that  $v_1 \rightarrow \langle \Delta_R \rangle$  and  $v_3 \rightarrow \langle \Delta_L \rangle$ .

The effective light neutrino mass, obtained this way is of the form

$$m_\nu \approx Y_L \langle \Delta_L \rangle - Y_\nu Y_R^{-1} Y_\nu^T \frac{\langle \Phi \rangle^2}{\langle \Delta_R \rangle} \quad (32)$$

We have the new vev seesaw relation

$$\langle \Delta_L \rangle \langle \Delta_R \rangle \sim \langle \Phi \rangle^2 \quad (33)$$

which naturally follows from minimization of the left-right symmetric scalar potential, together with the vev hierarchy

$$\langle \Delta_L \rangle \ll \langle \Phi \rangle \ll \langle \Delta_R \rangle \quad (34)$$

This implies, as before, that both type I and type II contributions vanish as  $\langle \Delta_R \rangle \rightarrow \infty$ . Notice that, strictly speaking, this version of left-symmetry is inconsistent with type-I seesaw [7] and requires the full form of the seesaw mass matrix [9, 10]. There are, however, tripletless left-right seesaw variants where a similar vev-seesaw formula holds, see Refs. [31–34] and Sec. 3.1.5.

If one can arrange for the breakdown of parity invariance to be spontaneous, then the smallness of neutrino masses gets correlated to the observed maximality of parity violation in low-energy weak interactions, as stressed by Mohapatra and Senjanovic [7]. However elegant this connection may be, it is phenomenologically not relevant, in view of the large value of the B-L scale. The latter is required both to fit the neutrino masses, as well as to unify the gauge couplings. Another important difference with respect to the simplest “1-2-3” seesaw is the absence of the majoron, which is now absorbed as the longitudinal mode of the gauge boson corresponding to the B-L generator which picks up a huge mass.

### 3.1.4 “Double” seesaw mechanism

One can add any number of (anomaly-free) gauge singlet leptons  $S_i$  to the SM, or any other gauge theory [9]. For example, in  $SO(10)$  and  $E(6)$  one may add leptons outside the **16** or the **27**, respectively. New important features may emerge when the seesaw is realized with non-minimal lepton content. Here we mention the seesaw scheme suggested in Ref. [29] motivated by string theories [30]. The model extends minimally the particle content of the SM by the sequential addition of a pair of two-component  $SU(3) \otimes SU(2) \otimes U(1)$  singlet leptons,  $\nu_i^c, S_i$ , with  $i$  a generation index running over

1, 2, 3. In the  $\nu, \nu^c, S$  basis, the  $9 \times 9$  neutral leptons mass matrix  $\mathcal{M}_\nu$  is given as

$$\mathcal{M}_\nu = \begin{pmatrix} 0 & Y_\nu^T \langle \Phi \rangle & 0 \\ Y_\nu \langle \Phi \rangle & 0 & M^T \\ 0 & M & \mu \end{pmatrix}, \quad (35)$$

in the basis  $\nu_L, \nu_L^c, S_L$ . Again  $Y_\nu$  is an arbitrary  $3 \times 3$  complex Yukawa matrix,  $M$  and  $\mu$  are  $SU(2)$  singlet complex mass matrices,  $\mu$  being symmetric. Notice that it has zeros in the  $\nu_L$ - $\nu_L$  and  $\nu_L^c$ - $\nu_L^c$  entries, a feature of several string models [30].

For  $\mu \gg M$  one has to first approximation that the  $S_i$  decouple leaving the simpler seesaw at scales below that. In such a “double” seesaw scheme the three light neutrino masses are determined from

$$m_\nu = \langle \Phi \rangle^2 Y_\nu^T M^{T-1} \mu M^{-1} Y_\nu, \quad (36)$$

The mass generation is illustrated in Fig. 3. A new feature is that there are two

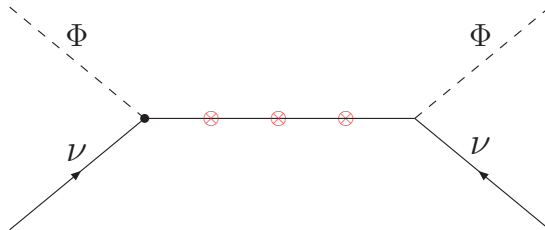


Figure 3: “Double” and “inverse” seesaw mechanism [29].

independent scales,  $\mu$  and  $M$ , of which only  $\mu$  breaks the B-L symmetry. Both scales can be large but, as we will see in Sec. 3.2.3, it is natural for  $\mu$  to be small [29], instead of large,  $\mu \ll M$ , see Sec. 3.2.3. For the case  $\mu = M$  one formally recovers the usual seesaw form, this is useful to present some results in simplified form, as used in Fig. 14.

Irrespective of what sets its scale, the entry  $\mu$  may be proportional to the vev of an  $SU(3) \otimes SU(2) \otimes U(1)$  singlet scalar, in which case the model contains a singlet majoron, see Sec. 5.4.1.

### 3.1.5 “Novel” $SO(10)$ seesaw mechanism

The seesaw is a mechanism which allows for many possible realizations. Schemes leading to the same pattern of neutrino masses may differ in many other respects. Correspondingly, there are many types of seesaw. In addition to type I [6,7] [11], type II [9,10], there are extended seesaw schemes, like type-III [31–33] and the double/inverse seesaw described above.

Here I turn to yet another seesaw that has recently been suggested in Ref. [34]. It belongs to the class of supersymmetric  $SO(10)$  models with broken D-parity. In addition to the states in the **16**, it contains three sequential gauge singlets  $S_{iL}$  with the following mass matrix

$$\mathcal{M}_\nu = \begin{pmatrix} 0 & Y_\nu \langle \Phi \rangle & F \langle \chi_L \rangle \\ Y_\nu^T \langle \Phi \rangle & 0 & \tilde{F} \langle \chi_R \rangle \\ F^T \langle \chi_L \rangle & \tilde{F}^T \langle \chi_R \rangle & 0 \end{pmatrix}, \quad (37)$$

in the same basis  $\nu_L, \nu_L^c, S_L$  as previously. Notice that it has zeros along the diagonal, specially in the  $\nu_L$ - $\nu_L$  and  $\nu_L^c$ - $\nu_L^c$  entries, thanks to the fact that there is no **126**, a feature of several string models [29, 30]. The resulting light neutrino mass matrix is

$$m_\nu \simeq \frac{\langle \Phi \rangle^2}{M_{\text{unif}}} \left[ Y_\nu (F \tilde{F}^{-1})^T + (F \tilde{F}^{-1}) Y_\nu^T \right] \quad (38)$$

where  $M_{\text{unif}}$  is the unification scale,  $F$  and  $\tilde{F}$  denote independent combinations of Yukawa couplings of the  $S_{iL}$ . One can see that the neutrino mass is suppressed by the unification scale  $M_{\text{unif}}$  *independently of the B-L breaking scale*. In contrast to all previous seesaws, this one is *linear* in the Dirac Yukawa couplings  $Y_\nu$ , as illustrated in Fig. 4. It is rather remarkable that one can indeed take the B-L scale as low as

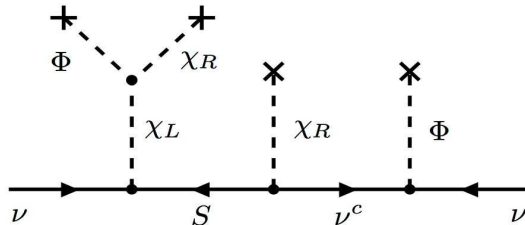


Figure 4: Low B-L scale  $SO(10)$  seesaw mechanism [34].

TeV without generating inconsistencies, neither with neutrino masses, nor with gauge coupling unification [34].

### 3.2 Low-scale models

There are many models of neutrino mass where the operator  $\mathcal{O}$  is induced from physics at accessible scales, TeV or less. The smallness of its strength may be naturally achieved due to loop and Yukawa couplings suppression. Moreover, the strength of the operator  $\mathcal{O}$  may be suppressed by small lepton number violating parameters that appear in its numerator, instead of its denominator, as commonly assumed. The latter correspond

to the seesaw-type schemes previously discussed. The former correspond to the class we are about to describe. Before I do so, let me emphasize that such models are also “natural” in t’Hooft’s sense [35]: “*an otherwise arbitrary parameter may be taken as small when the symmetry of the Lagrangean increases by having it vanish*”.

Since all particles are at the TeV scale, these models naturally lead to possibly testable phenomenological implications, including lepton flavour violation and modifications in muon and tau decays.

Moreover, when the breaking of lepton number entailed in these models takes place spontaneously, the corresponding Goldstone boson has a remarkable property: it may couple substantially to the SM Higgs boson, which can therefore have a sizeable invisible decay branching ratio [36–39]

$$H \rightarrow JJ \tag{39}$$

where  $J$  is the majoron. This shows that, although neutrino masses are small, the neutrino mass generation may have very important implications for the mechanism of electroweak symmetry breaking. One must therefore take into account the existence of the invisible channel in designing Higgs boson search strategies at future collider experiments [40, 41]. Further discussion in Sec. 5.4.1.

### 3.2.1 Radiative models

Neutrino masses may be induced by calculable radiative corrections [42]. For example, they can arise at the two-loop level [43] as illustrated in Fig. 5. Up to a logarithmic factor one has, schematically,

$$\mathcal{M}_\nu \sim \lambda_0 \left( \frac{1}{16\pi^2} \right)^2 f Y_l h Y_l f^T \frac{\langle \Phi \rangle^2}{(m_k)^2} \langle \sigma \rangle \tag{40}$$

in the limit where the doubly-charged scalar  $k$  is much heavier than the singly charged one. Here  $l$  denotes a charged lepton,  $f$  and  $h$  are their Yukawa coupling matrices and  $Y_l$  denotes the SM Higgs Yukawa couplings to charged leptons. Here  $\langle \sigma \rangle$  denotes an  $SU(3) \otimes SU(2) \otimes U(1)$  singlet vev used in Ref. [44]. Clearly, even if the proportionality factor  $\lambda_0$  is large, the neutrino mass can be made naturally small by the presence of a product of five small Yukawas and the appearance of the two-loop factor.

### 3.2.2 Supersymmetry and neutrino mass

Low energy supersymmetry can be the origin of neutrino mass [45]. The intrinsically supersymmetric way to break lepton number is to break the so-called R parity. This

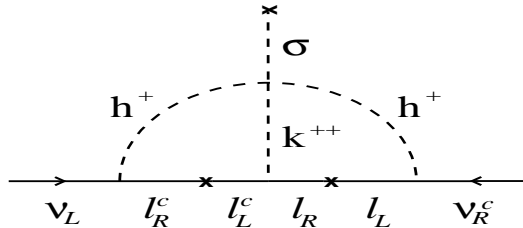


Figure 5: Two-loop origin for neutrino mass [43, 44].

could happen spontaneously, driven by a nonzero vev of an  $SU(3) \otimes SU(2) \otimes U(1)$  singlet sneutrino [46–48], and leads to an effective model characterized by purely bilinear R parity violation [49]. This also serves as reference model, as it provides the minimal way to add neutrino masses to the MSSM, we call it RMSSM. Neutrino mass generation takes place in a hybrid scenario, with one scale generated at tree level and the other induced by “calculable” radiative corrections [50]. Here the two blobs in the graph

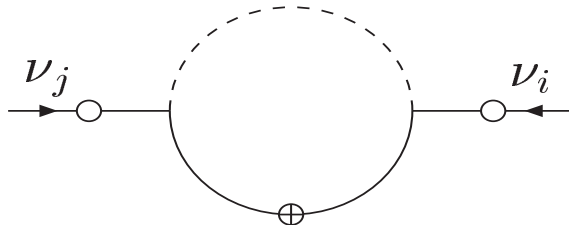


Figure 6: Loop origin of solar mass scale in RMSSM [50].

Fig. 6 denote  $\Delta L = 1$  insertions, while the crossed blob accounts for chirality flipping, and  $A$  denotes the trilinear soft supersymmetry breaking coupling. The general form of the expression is quite involved but the approximation

$$\mathcal{M}_\nu \sim \left( \frac{1}{16\pi^2} \right) \langle \Phi \rangle^2 \frac{A}{m_0} Y_d Y_d \quad (41)$$

holds in some regions of parameters. The neutrino mass spectrum naturally follows a normal hierarchy, with the atmospheric scale generated at the tree level and the solar mass scale arising from calculable loops.

### 3.2.3 “Inverse” seesaw mechanism

Here we mention that there are also low-scale tree-level neutrino mass schemes with naturally light neutrinos. One is the inverse seesaw scheme suggested in [29] and already described in Sec. 3.1.4. The mass matrix is the same as that of the double

seesaw model, given in eq. (35). The only difference is that now the entry  $\mu$  is taken very small, e. g.  $\mu \ll Y_\nu \langle \phi \rangle \ll M$  [29]. Notice that for small  $\mu$  neutrino masses vanish with  $\mu$ ,

$$m_\nu = \langle \Phi \rangle^2 Y_\nu^T M^{T-1} \mu M^{-1} Y_\nu$$

as illustrated in Fig. 3.

The fact that the neutrino mass vanishes as  $\mu \rightarrow 0$  is just the opposite of the behaviour of the seesaw formulas in Eqs. (27) (30) and (32); thus this is sometimes called *inverse* seesaw model of neutrino masses. The entry  $\mu$  may be proportional to the vev of an SU(2) singlet scalar, in which case spontaneous B-L violation leads to the existence of a majoron [51]. This would be characterized by a relatively low scale, so that the corresponding phase transition could take place after the electroweak transition. The naturalness of the model stems from the fact that in the limit when  $\mu \rightarrow 0$  lepton number is recovered, increasing the symmetry of the theory.

## 4 The lepton mixing matrix

In any gauge theory in order to identify physical particles one must diagonalize all relevant mass matrices, which typically result from gauge symmetry breaking. Mechanisms giving mass to neutrinos generally imply the need for new interactions whose Yukawas (like  $Y_\nu$  in seesaw-type schemes) will coexist with that of the charged leptons,  $Y_l$ . Since in general these are independent one has that, like quarks, massive neutrinos generally mix. The structure of this mixing is not generally predicted from first principles. Whatever the ultimate high energy gauge theory may be it must be broken to the SM at low scales, so one should characterize the structure of the lepton mixing matrix in terms of the  $SU(3) \otimes SU(2) \otimes U(1)$  structure. The procedure is the familiar one from the quark sector.

### 4.1 Dirac case

Here we derive the structure of the lepton mixing matrix of massive Dirac neutrinos and its parametrization, as presented in Ref. [9]. From the start  $V$  can be parametrized as

$$V = \omega_0(\gamma) \prod_{i < j}^n \omega_{ij}(\eta_{ij}) \quad (42)$$

where

$$\omega_0(\gamma) = \exp i \left( \sum_{a=1}^n \gamma_a A_a^a \right)$$

is a diagonal unitary ‘‘Cartan’’ matrix, described by  $n - 1$  real parameters  $\gamma_a$ <sup>1</sup>. On the other hand each factor

$$\omega_{ab}(\eta_{ab}) = \exp \sum_{a=1}^n (\eta_{ab} A_a^b - \eta_{ab}^* A_b^a)$$

is a complex rotation in  $ab$  with parameter  $\eta_{ab} = |\eta_{ab}| \exp i\theta_{ab}$ . For example,

$$\omega_{12}(\eta_{12}) = \begin{pmatrix} c_{12} & e^{i\phi_{12}} s_{12} & 0 & \dots \\ -e^{-i\phi_{12}} s_{12} & c_{12} & 0 & \dots \\ 0 & 0 & 1 & \dots \\ \dots & \dots & \dots & \dots \end{pmatrix} \quad (43)$$

Once the charged leptons and Dirac neutrino mass matrices are diagonal, one can still rephase the corresponding fields by  $\omega_0(\alpha)$  and  $\omega_0(\gamma - \alpha)$ , respectively, keeping invariant the form of the free Lagrangean. This results in the form

$$V = \omega_0(\alpha) \prod_{i < j}^n \omega_{ij}(\eta_{ij}) \omega_0^\dagger(\alpha), \quad (44)$$

where we are still free to choose the  $n - 1$   $\alpha$ -values associated to Dirac neutrino phase redefinitions. Using the conjugation property

$$\omega_0(\alpha) \omega_{ab}(|\eta_{ab}| \exp i\theta_{ab}) \omega_0^\dagger(\alpha) = \omega_{ab}[|\eta_{ab}| \exp i(\alpha_a + \theta_{ab} - \alpha_b)] \quad (45)$$

we arrive at the final Dirac lepton mixing matrix which is, of course, identical in form to that describing quark mixing. It involves a set of

$$n(n - 1)/2 \text{ mixing angles } \theta_{ij} \text{ and } n(n - 1)/2 - (n - 1) \text{ CP phases.} \quad (46)$$

where  $(n - 1)$  phases were eliminated. This is the parametrization as originally given in Ref. [9], with unspecified factor ordering. From Eq. (46) one sees that for  $n = 3$  there are 3 angles and precisely one leptonic CP violating phase, just as in the Kobayashi-Maskawa matrix describing quark mixing. Two of the three angles are involved in solar

---

<sup>1</sup>By choosing an overall relative phase between charged leptons and Dirac neutrinos we can take  $V$  as unimodular, i. e.  $\det V = 1$ , so that  $\sum_{a=1}^n \gamma_a = 1$ .

and atmospheric oscillations, so we set  $\theta_{12} \equiv \theta_{\text{SOL}}$  and  $\theta_{23} \equiv \theta_{\text{ATM}}$ . The last angle in the three-neutrino leptonic mixing matrix is  $\theta_{13}$ ,

$$\omega_{13} = \begin{pmatrix} c_{13} & 0 & e^{i\Phi_{13}} s_{13} \\ 0 & 1 & 0 \\ -e^{-i\Phi_{13}} s_{13} & 0 & c_{13} \end{pmatrix}. \quad (47)$$

A convenient ordering prescription is to take  $\mathbf{23} \times \mathbf{13} \times \mathbf{12}$ , or “atmospheric”  $\times$  “reactor”  $\times$  “solar”, with the phase being associated to  $\theta_{13}$ . In summary, if neutrino masses are added *a la Dirac* their charged current weak interaction has exactly the same structure as that of quarks.

## 4.2 Majorana case

Here we consider the form of the lepton mixing matrix in models where neutrino masses arise in the absence of right-handed neutrinos, such as those in Sec. 3.2.1. The unitary form also holds, to a good approximation, to models where SU(2) doublet neutrinos mix only slightly with other states, like high-scale seesaw models.

For  $n$  generations of Majorana neutrinos the lepton mixing matrix has exactly the same form given in Eq. (44). The difference is that in the case of Majorana neutrinos their mass term is manifestly not invariant under rephasings of the neutrino fields. As a result, the parameters  $\alpha$  in Eq. (44) can *not* be used to eliminate  $n - 1$  Majorana phases as we just did in Sec. 4.1. Consequently these are additional phases [9] which show up in L-violating processes [19, 20]. Such new sources of CP violation in gauge theories with Majorana neutrinos are called “Majorana phases”. They already exist in a theory with just two generations of Majorana neutrinos [9],  $n = 2$ , whose mixing matrix is described by

$$\omega_{13} = \begin{pmatrix} c_{12} & e^{i\Phi_{12}} s_{12} \\ -e^{-i\Phi_{12}} s_{12} & c_{12} \end{pmatrix}, \quad (48)$$

where  $\phi_{12}$  is the Majorana phase (recall that Cabibbo mixing has no CP phase). Such “Majorana” CP phases are, in a sense, mathematically more “fundamental” than the Dirac phase, whose existence, as we just saw, requires at least three generations.

For the case of three neutrinos the lepton mixing matrix can be parametrized as [9]

$$K = \omega_{23}\omega_{13}\omega_{12} \quad (49)$$

where each factor in the product of the  $\omega$ ’s is effectively  $2 \times 2$ , characterized by an angle and a CP phase. Such symmetrical parameterization of the lepton mixing matrix,  $K$

can be written as:

$$\begin{bmatrix} c_{12}c_{13} & s_{12}c_{13}e^{i\phi_{12}} & s_{13}e^{i\phi_{13}} \\ -s_{12}c_{23}e^{-i\phi_{12}} - c_{12}s_{13}s_{23}e^{i(\phi_{23}-\phi_{13})} & c_{12}c_{23} - s_{12}s_{13}s_{23}e^{i(\phi_{12}+\phi_{23}-\phi_{13})} & c_{13}s_{23}e^{i\phi_{23}} \\ s_{12}s_{23}e^{-i(\phi_{12}+\phi_{23})} - c_{12}s_{13}c_{23}e^{-i\phi_{13}} & -c_{12}s_{23}e^{-i\phi_{23}} - s_{12}s_{13}c_{23}e^{i(\phi_{12}-\phi_{13})} & c_{13}c_{23} \end{bmatrix}.$$

All three CP phases are physical [19]:  $\phi_{12}$ ,  $\phi_{23}$  and  $\phi_{13}$ . The “invariant” combination  $\delta = \phi_{12} + \phi_{23} - \phi_{13}$  corresponds to the “Dirac phase”. If neutrinos are of Dirac type, only a single phase (say  $\phi_{13}$ ) may be taken to be non-zero. This phase corresponds to the phase present in the Kobayashi-Maskawa matrix, and this is the one that affects neutrino oscillations. The other two phases are associated to the Majorana nature of neutrinos and show up only in lepton-number violating processes, like neutrinoless double beta decay [19, 20].

An important subtlety arises regarding the conditions for CP conservation in gauge theories of massive Majorana neutrinos. Unlike the case of Dirac fermions, where CP invariance implies that the mixing matrix should be real, in the Majorana case the condition is [21]

$$K^* = K\eta$$

where  $\eta = \text{diag}(+, +, \dots, , , \dots)$  is the signature matrix describing the relative signs of the neutrino mass eigenvalues that follow from diagonalizing the relevant Majorana mass matrix, if one chooses to use real diagonalizing matrices [22]. Consequently say, for  $n = 2$ , both  $\phi_{12} = \pi/2$  and  $\phi_{12} = 0$  correspond to CP conservation, as emphasized by Wolfenstein. These important signs determine the CP properties of the neutrinos and play a crucial role in  $0\nu\beta\beta$ .

### 4.3 Seesaw-type mixing

The most general theory of neutrino mass is effectively described in SM terms by  $(n, m)$ ,  $n$  being the number of  $SU(3) \otimes SU(2) \otimes U(1)$  isodoublets and  $m \neq 0$  the number of  $SU(3) \otimes SU(2) \otimes U(1)$  isosinglet two-component leptons (the case  $m = 0$  was given above). Here we assume an arbitrary number of gauge singlets, since they carry no anomaly. The usual seesaw in Secs. 3.1.1, 3.1.2 and 3.1.3 has  $m = n = 3$ , while the extended seesaw in Secs. 3.1.4, 3.1.5 and 3.2.3 have  $m = 2n = 6$ . Isosinglets have in general a gauge and Lorentz invariant Majorana mass term. The procedure holds in any scheme of Majorana neutrino masses where isosinglet and isodoublet mass terms coexist [9].

The effective form of such a “seesaw” lepton mixing matrix has, in addition to Majorana phases, many doublet-singlet mixing parameters, in general complex [9]. Its general structure is substantially more complex than “usual”, being described by a rectangular matrix, called  $K$ . As a result one finds that leptonic mixing as well as CP violation may take place even in the massless neutrino limit [52, 53].

The existence of these neutral heavy leptons could be inferred from low energy weak decay processes, where the neutrinos that can be kinematically produced are only the light ones. The mixing matrix describing the charged weak interactions of the light (mass-eigenstate) neutrinos is effectively non-unitary, since the coupling of a given light neutrino to the corresponding charged lepton is decreased by a certain factor associated with the heavy neutrino coupling. There are constraints on the strength of the such mixing matrix elements that follow from weak universality and low energy weak decay measurements, as well as from LEP.

The full weak charged current mixing matrix  $K$  of the general  $(n, m)$  models involves

$$n(n + 2m - 1)/2 \text{ mixing angles } \theta_{ij} \quad \text{and} \quad n(n + 2m - 1)/2 \text{ CP phases } \phi_{ij}. \quad (50)$$

For the explicit parametrization the reader is referred to the original paper, Ref. [9]. One sees that, for example, the usual seesaw model [labeled (3, 3) in our language] is characterized by 12 mixing angles and 12 CP phases (both Dirac and Majorana-type) [9].

This number far exceeds the corresponding number of parameters describing the charged current weak interaction of quarks. As already mentioned, the reason is twofold: (i) neutrinos are Majorana particles, their mass terms are not invariant under rephasings, and (ii) the isodoublet neutrinos in general mix with the  $SU(3) \otimes SU(2) \otimes U(1)$  singlets. As a result, there are far more physical CP phases that may play a role in neutrino oscillations and/or leptogenesis (see below).

Another important feature which arises in any theory based on  $SU(3) \otimes SU(2) \otimes U(1)$  where isosinglet and isodoublet lepton mass terms coexist is that the leptonic neutral current is non-trivial [9]: there are non-diagonal couplings of the Z to the mass-eigenstate neutrinos. They are expressed as a projective hermitian matrix

$$P = K^\dagger K.$$

This contrasts with the neutral current couplings of mass-eigenstate neutrinos in schemes where lepton number is conserved (Sec. 4.1) or where no isosinglet leptons are present,

i.e.,  $m = 0$  (Sec. 4.2). In both cases, just as for quarks, the neutral current couplings are diagonal (Glashow-Iliopoulos-Maiani mechanism).

Before we close, note that, in a scheme with  $m < n$ ,  $n - m$  neutrinos will remain massless, while  $2m$  neutrinos will acquire Majorana masses,  $m$  light and  $m$  heavy [9]. For example, in a model with  $n = 3$  and  $m = 1$  one has one light and one heavy Majorana neutrino, in addition to the two massless ones. In this case clearly there will be less parameters than present in a model with  $m = n$ .

## 5 Phenomenology

Obviously the first phenomenological implication of neutrino mass models is the phenomenon of neutrino oscillations, required to account for the current solar and atmospheric neutrino data. The interpretation of the data relies on good calculations of the corresponding fluxes [54,55], neutrino cross sections and response functions, as well as on an accurate description of neutrino propagation in the Sun and the Earth, taking into account matter effects [56,57].

### 5.1 Status of neutrino oscillations

Current neutrino oscillation data have no sensitivity to CP violation. Thus we neglect all phases in the analysis and take, moreover, the simplest unitary 3-dimensional form of the lepton mixing matrix in Eq. (49) with the three phases set to zero. In this approximation oscillations depend on the three mixing parameters  $\sin^2 \theta_{12}$ ,  $\sin^2 \theta_{23}$ ,  $\sin^2 \theta_{13}$  and on the two mass-squared splittings  $\Delta m_{\text{SOL}}^2 \equiv \Delta m_{21}^2 \equiv m_2^2 - m_1^2$  and  $\Delta m_{\text{ATM}}^2 \equiv \Delta m_{31}^2 \equiv m_3^2 - m_1^2$  characterizing solar and atmospheric neutrinos. The hierarchy  $\Delta m_{\text{SOL}}^2 \ll \Delta m_{\text{ATM}}^2$  implies that one can set  $\Delta m_{\text{SOL}}^2 = 0$ , to a good approximation, in the analysis of atmospheric and accelerator data. Similarly, one can set  $\Delta m_{\text{ATM}}^2$  to infinity in the analysis of solar and reactor data.

The world's neutrino oscillation data and their analysis, as of June 2006, are given in Ref. [14] and will not be repeated here. The new developments are: new Standard Solar Model [58], new SNO salt data [59], latest K2K [60] and MINOS [61] data. These are briefly described in Appendix C of hep-ph/0405172 (v5). In what follows we summarize the updated results of the analysis which takes into account all these new data. Apart from the “positive” data already mentioned, the analysis also includes the constraints from “negative” oscillation searches at reactor experiments, CHOOZ and Palo Verde.

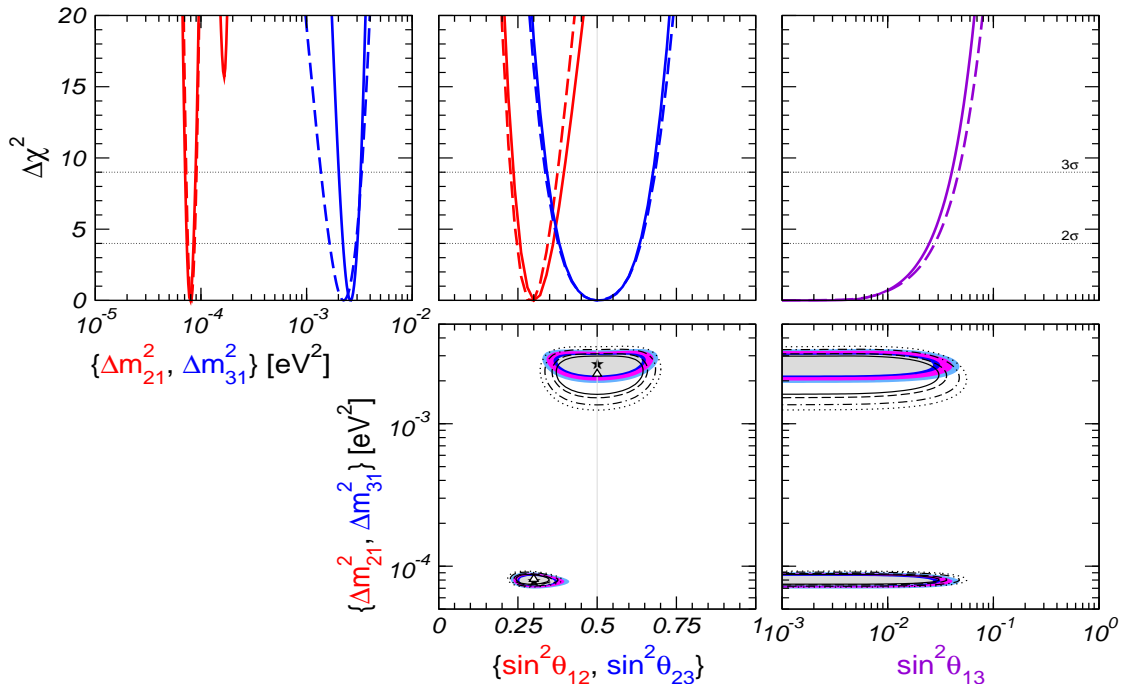


Figure 7: Three–neutrino regions allowed by the world’s neutrino oscillation data at 90%, 95%, 99%, and  $3\sigma$  C.L. for 2 d.o.f. as of June 2006, from Ref. [14]. In top panels  $\Delta\chi^2$  is minimized with respect to undisplayed parameters.

The three–neutrino oscillation parameters that follow from the global oscillation analysis in Ref. [14] are summarized in Fig. 7. In the upper panels of the figure the  $\Delta\chi^2$  is shown as a function of the three mixing parameters  $\sin^2\theta_{12}$ ,  $\sin^2\theta_{23}$ ,  $\sin^2\theta_{13}$  and two mass squared splittings  $\Delta m_{21}^2, \Delta m_{31}^2$ , minimized with respect to the undisplayed parameters. The lower panels show two-dimensional projections of the allowed regions in the five-dimensional parameter space. In addition to a confirmation of oscillations with  $\Delta m_{\text{ATM}}^2$ , accelerator neutrinos provide a better determination of  $\Delta m_{\text{ATM}}^2$ . For example, comparing dashed and solid lines in Fig. 7 one sees that the inclusion of the new data (mainly MINOS [61]) leads to a slight increase in  $\Delta m_{\text{ATM}}^2$  and an improvement on its determination (see [14] for details). On the other hand reactors [3] have played a crucial role in selecting large-mixing-angle (LMA) oscillations [62] out of the previous “zoo” of solutions [63]. The best fit values and the allowed  $3\sigma$  ranges of the oscillation parameters from the global data are summarized in Table 2.

Note that in a three–neutrino scheme CP violation disappears when two neutrinos become degenerate or when one of the angles vanishes [64]. As a result CP violation is doubly suppressed, first by  $\alpha \equiv \Delta m_{\text{SOL}}^2 / \Delta m_{\text{ATM}}^2$  and also by the small mixing angle  $\theta_{13}$ . The left panel in Fig. 8 gives the parameter  $\alpha$ , as determined from the global  $\chi^2$

parameter	best fit	$3\sigma$ range
$\Delta m_{21}^2$ [ $10^{-5}$ eV $^2$ ]	7.9	7.1–8.9
$\Delta m_{31}^2$ [ $10^{-3}$ eV $^2$ ]	2.6	2.0–3.2
$\sin^2 \theta_{12}$	0.30	0.24–0.40
$\sin^2 \theta_{23}$	0.50	0.34–0.68
$\sin^2 \theta_{13}$	0.00	$\leq 0.040$

Table 2: Neutrino oscillation parameters as of June 2006, from Ref. [14].

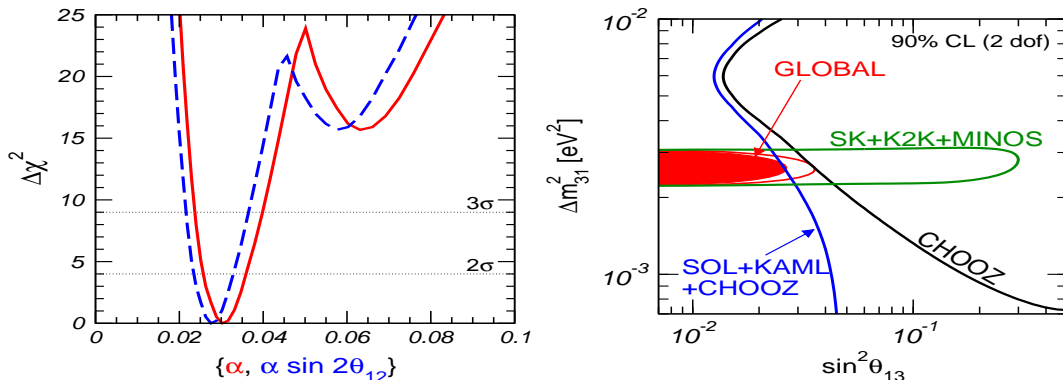


Figure 8: Determination of  $\alpha \equiv \Delta m_{\text{SOL}}^2 / \Delta m_{\text{ATM}}^2$  and bound on  $\sin^2 \theta_{13}$  from data, as of June 2006, from Ref. [14].

analysis. The right panel shows the impact of different data samples on constraining  $\theta_{13}$ . One sees that, although for larger  $\Delta m_{\text{ATM}}^2$  values the bound on  $\sin^2 \theta_{13}$  is dominated by CHOOZ, this bound deteriorates quickly as  $\Delta m_{\text{ATM}}^2$  decreases (see Fig. 8), so that the solar and KamLAND data become relevant.

There is now a strong ongoing effort aimed at probing  $\theta_{13}$  and CP violation in future neutrino oscillation searches at reactors and accelerators [65–67]. As we saw, the basic parameters  $\alpha \equiv \Delta m_{\text{SOL}}^2 / \Delta m_{\text{ATM}}^2$  and  $\sin^2 \theta_{13}$  characterizing the strength of CP violation in neutrino oscillations are small. Prospects for probing  $\sin^2 \theta_{13}$  at long baseline reactor and accelerator neutrino oscillation experiments are given in Ref. [68],

Information on  $\sin^2 \theta_{13}$  may also come from a totally different class of studies of the day/night effect in large water Cerenkov solar neutrino experiments such as UNO or Hyper-K [69] [70].

## 5.2 Predicting neutrino masses and mixing

Gauge symmetry alone is not sufficient to predict particle mixings, neither for the quarks, nor for the leptons: such “flavour problem” has remained with us for a while.

As we saw in Sec. 5.1 five of the basic parameters of the lepton sector are currently probed in neutrino oscillation studies. These point towards a well defined pattern of neutrino mixing angles, quite distinct from that of quarks. Such pattern is not easy to account for in the context of unified schemes where quarks and leptons are connected. The data seem to indicate an intriguing complementarity between quark and lepton mixing angles [71–74].

There has been a rush of papers attempting to understand the values of the leptonic mixing angles from underlying symmetries at a fundamental level. For example the following form of the neutrino mixing angles has been proposed [75]

$$\begin{aligned}\tan^2 \theta_{\text{ATM}} &= \tan^2 \theta_{23}^0 = 1 \\ \sin^2 \theta_{\text{Chooz}} &= \sin^2 \theta_{13}^0 = 0 \\ \tan^2 \theta_{\text{sol}} &= \tan^2 \theta_{12}^0 = 0.5.\end{aligned}\tag{51}$$

Such Harrison-Perkins-Scott pattern [76] could result from some kind of flavour symmetry, valid at a very high energy scale where the dimension-five neutrino mass operator arises.

One approach to predict neutrino masses and mixing angles was the idea that neutrino masses arise from a common seed at some “neutrino mass unification” scale  $M_X$  [77], very similar the merging of the SM gauge coupling constants at high energies due to supersymmetry [78]. However, in its simplest form this very simple theoretical ansatz is now inconsistent (at least if CP is conserved) with the current observed value of the solar mixing angle  $\theta_{12}$  inferred from current data.

A more satisfactory and fully viable alternative realization of the “neutrino mass unification” idea employs an  $A_4$  flavour symmetry introduced by Ernest Ma, in the context of a seesaw scheme [79]. Starting from three-fold degeneracy of the neutrino masses at a high energy scale, a viable low energy neutrino mass matrix can indeed be obtained in agreement with neutrino data as well as constraints on lepton flavour violation in  $\mu$  and  $\tau$  decays. The model predicts maximal atmospheric angle and vanishing  $\theta_{13}$ ,

$$\theta_{23} = \pi/4 \quad \text{and} \quad \theta_{13} = 0.$$

Although the solar angle  $\theta_{12}$  is unpredicted, one expects <sup>2</sup>

$$\theta_{12} = \mathcal{O}(1).$$

When CP is violated  $\theta_{13}$  becomes arbitrary and the Dirac phase is maximal [81].

Within such flavour symmetric seesaw scheme one can show that the lepton and slepton mixings are intimately related. The resulting slepton spectrum must necessarily include at least one mass eigenstate below 200 GeV, which can be produced at the LHC. The prediction for the absolute Majorana neutrino mass scale  $m_0 \geq 0.3$  eV ensures that the model will be tested by future cosmological tests and  $\beta\beta_{0\nu}$  searches. Rates for lepton flavour violating processes  $l_j \rightarrow l_i + \gamma$  typically lie in the range of sensitivity of coming experiments, with  $\text{BR}(\mu \rightarrow e\gamma) \gtrsim 10^{-15}$  and  $\text{BR}(\tau \rightarrow \mu\gamma) > 10^{-9}$ .

Finally, we mention that there have been attempts to realize the Harrison-Perkins-Scott mixing pattern in Eq. (51) at some high energy scale, and to correct its predictions by renormalization group evolution [82, 83]. For a survey of related attempts see Ref. [84].

### 5.3 Absolute scale of neutrino mass and $0\nu\beta\beta$

Neutrino oscillations are blind to whether neutrinos are Dirac or Majorana. As we have seen, on general grounds, neutrinos are expected to be Majorana [9]. Neutrinoless double beta decay and other lepton number violation processes, such as neutrino transition electromagnetic moments [21, 22] [85, 86] are able to probe the basic nature of neutrinos.

The significance of neutrinoless double beta decay stems from the fact that, in a gauge theory, irrespective of the mechanism that induces  $0\nu\beta\beta$ , it necessarily implies a Majorana neutrino mass [17], as illustrated in Fig. 9. Thus it is a basic issue. Quantitative implications of the “black-box” argument are model-dependent, but the theorem itself holds in any “natural” gauge theory.

Conventional neutrino oscillations are also insensitive to the absolute scale of neutrino masses [18–20]. Although the latter will be tested directly in high sensitivity tritium beta decay studies [87], as well as by its effect on the cosmic microwave background and the large scale structure of the Universe [88–90]  $0\nu\beta\beta$  may give valuable complementary information. For example, as seen above, the  $A_4$  model [79] gives a lower bound on the absolute Majorana neutrino mass  $m_\nu \gtrsim 0.3$  eV and may therefore be tested in  $0\nu\beta\beta$  searches.

---

<sup>2</sup>There have been realizations of the  $A_4$  symmetry that also predict the solar angle, e. g. Ref. [80].

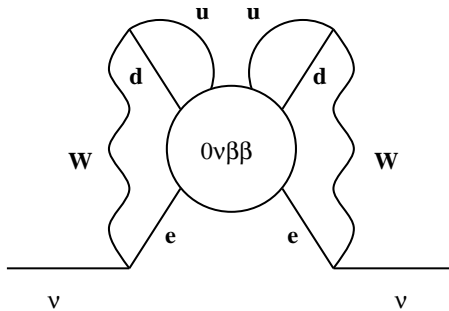


Figure 9: Neutrinoless double beta decay and Majorana mass are equivalent [17].

Now that oscillations are experimentally confirmed we know that  $0\nu\beta\beta$  must be induced by the exchange of light Majorana neutrinos, the so-called "mass-mechanism". The corresponding amplitude is sensitive [19,20] both to the absolute scale of neutrino mass, as well as to Majorana phases [9], neither of which can be probed in oscillations [18,19].

Fig. 10 shows the estimated average mass parameter characterizing the neutrino exchange contribution to  $0\nu\beta\beta$  versus the lightest and heaviest neutrino masses. The calculation takes into account the current neutrino oscillation parameters in [14] and state-of-the-art nuclear matrix elements [91]. The upper (lower) panel corresponds to the cases of normal (inverted) neutrino mass spectra. In these plots the "diagonals" correspond to the case of quasi-degenerate neutrinos [79] [92] [93]. In the normal hierarchy case there is in general no lower bound on the  $\beta\beta_{0\nu}$  rate since there can be a destructive interference amongst the neutrino amplitudes. In contrast, the inverted neutrino mass hierarchy implies a "lower" bound for the  $\beta\beta_{0\nu}$  amplitude. A specific normal hierarchy model for which a lower bound on  $\beta\beta_{0\nu}$  can be placed has been given in Ref. [80]. An interesting feature is that such lower bound depends, as expected, on the value of the Majorana violating phase  $\phi_1$ , as indicated in Fig. 11.

The best current limit on  $\langle m_\nu \rangle$  comes from the Heidelberg-Moscow experiment. There is also a claim made in Ref. [94] (see also Ref. [95]) which will be important to confirm or refute in future experiments. GERDA will provide an independent check of this claim [96]. SuperNEMO, CUORE, EXO, MAJORANA and possibly other experiments will further extend the sensitivity of current  $\beta\beta_{0\nu}$  searches [97].

## 5.4 Other phenomena

If neutrino masses arise *a la* seesaw the dynamics responsible for generating the small neutrino masses seems most likely untestable. In other words, beyond neutrino masses

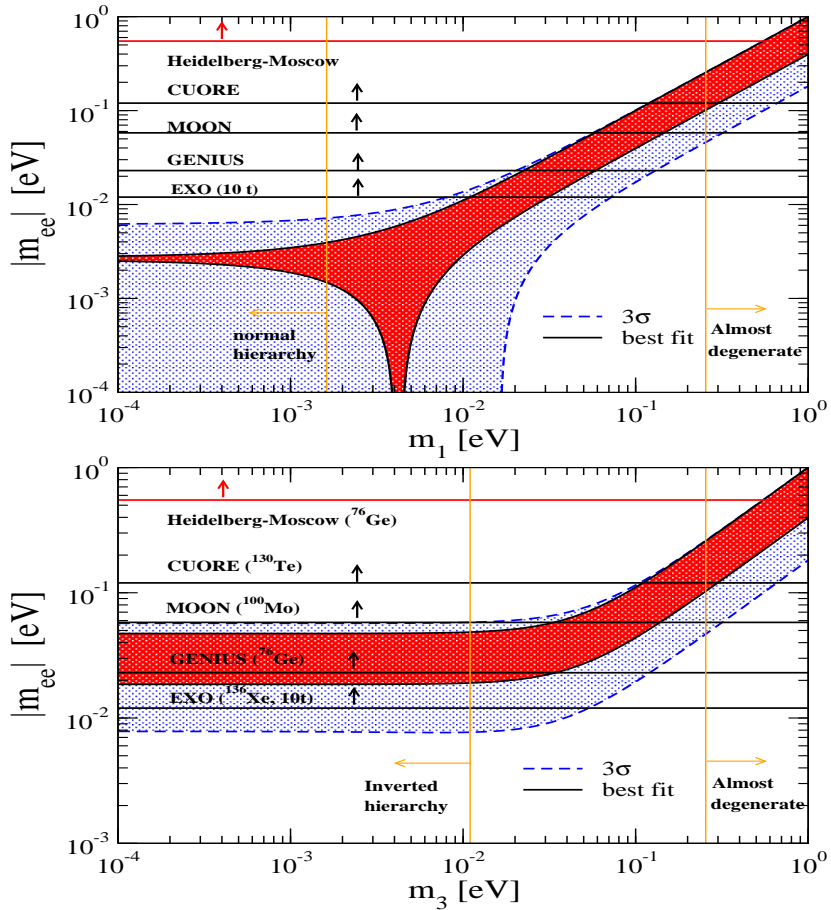


Figure 10:  $0\nu\beta\beta$  amplitude versus current oscillation data, from Ref. [91].

and oscillations, theories can not be probed phenomenologically at low energies, due to the large scale involved. However when the breaking of lepton number symmetry is spontaneous there is a dynamical “tracer” of the mass-generation mechanism which might be probed experimentally.

#### 5.4.1 Majoron physics

If neutrino masses follow from spontaneous violation of global lepton number, the existence of the Goldstone boson brings new interactions for neutrinos and Higgs boson(s) which may lead to new phenomena. While neither of these is expected within the usual high-scale seesaw schemes, both could lead to detectable signals in low-scale models of neutrino mass.

As already mentioned, the majoron may couple substantially to the SM Higgs boson, which can therefore have a sizeable decay branching ratio [36–39] into the channel in eq. (39). Such “invisible” channel is experimentally detectable as missing energy or

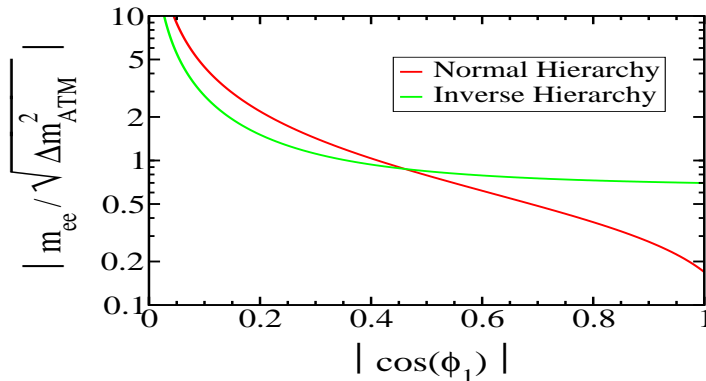


Figure 11: Lower bound on  $|\langle m_{ee} \rangle| / \Delta m_{\text{ATM}}^2$  vs  $|\cos(\phi_1)|$  where  $\phi_1$  is a Majorana phase in the model of Ref. [80]. The lines in dark (red) and grey (green) correspond to normal and inverse hierarchy.

transverse momentum associated to the Higgs [40, 41]. Therefore in low-scale models of neutrino mass the neutrino mass-giving mechanism may have a strong impact in the electroweak sector.

Majoron-emitting neutrino decays can also lead to detectable signals in low-scale models of neutrino mass,

$$\nu_3 \rightarrow \nu + J,$$

For example, if the neutrinos decay in high density media, like supernovae, characterized by huge matter densities, then the “matter-assisted” decays would lead to detectable signals in underground water Cerenkov experiments [98].

#### 5.4.2 New gauge boson

Although in the usual large-scale seesaw with gauged B-L symmetry, there are new gauge bosons associated to the neutrino mass generation these are too heavy to give any detectable effect. Only when the B-L scale is low, as in the model discussed in Sec. 3.1.5 or the model considered in Ref. [99], there will exist a light new neutral gauge boson,  $Z'$  that could be detected in searches for Drell-Yan processes at the LHC.

#### 5.4.3 Lepton flavour violation

In the presence of supersymmetry, seesaw phenomenology is richer. A generic feature of supersymmetric seesaw models is the existence of processes with lepton flavour violation such as  $\mu^- \rightarrow e^- \gamma$ . Supersymmetry contributes through the exchange of charginos (neutralinos) and sneutrinos (charged sleptons) [100–102], as illustrated in Fig. 12.



Figure 12: Supersymmetric Feynman diagrams for  $l_i^- \rightarrow l_j^- \gamma$ .

Similarly the nuclear  $\mu^- - e^-$  conversion arises, as indicated in Fig. 13. The rates for

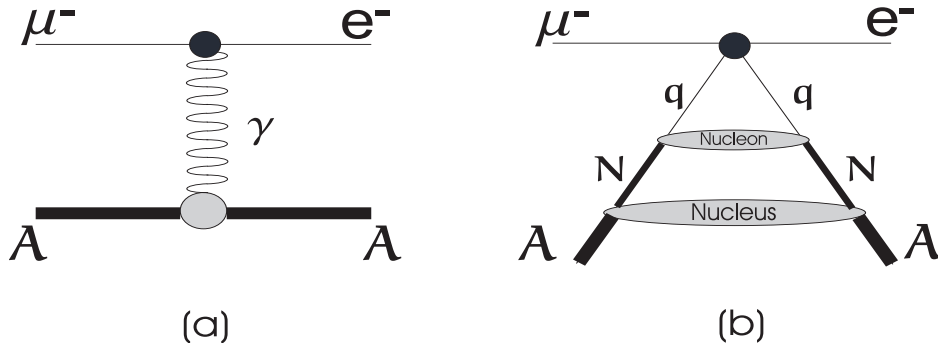


Figure 13: Contributions to the nuclear  $\mu^- - e^-$  conversion: (a) long-distance and (b) short-distance. For numerical results see Ref. [108]

these process can both be sizeable. As an example, consider the rates for the  $\mu^- \rightarrow e^- \gamma$  decay, given in Fig. 14.

The calculation leading to Fig. 14 is done in the framework of the supersymmetric double/inverse seesaw model in Secs. 3.1.4 and 3.2.3 [103]. This allows one to analyse the interplay of neutral heavy lepton [104]<sup>3</sup> and supersymmetric contributions [102]. The figure shows the  $Br(\mu \rightarrow e \gamma)$  contours in the  $(M, \frac{\mu}{M})$ -plane (logarithmic scales) for hierarchical light neutrinos with  $m_1 = 0$  eV (left panel) and for degenerate light neutrinos with  $m_1 = 0.3$  eV (right panel). The shaded contours correspond to (from left to right):  $Br(\mu \rightarrow e \gamma) = 10^{-15, -13, -11, -9}$ . For large  $M$  the estimates are similar to those of the standard supersymmetric seesaw. However, if the neutral heavy leptons are in the TeV range (a situation not realizable in the minimal seesaw mechanism), the  $Br(\mu \rightarrow e \gamma)$  rate can be enhanced even in the *absence* of supersymmetry. This is indicated by the contours in the lower left, which depict the contribution from neutral heavy leptons only. For such  $M$  values around TeV or so, the quasi-Dirac neutral heavy leptons may

<sup>3</sup>Since in this model flavor and CP violation can occur in the massless neutrino limit, the allowed rates are unsuppressed by the smallness of neutrino masses [52, 53, 104–106].

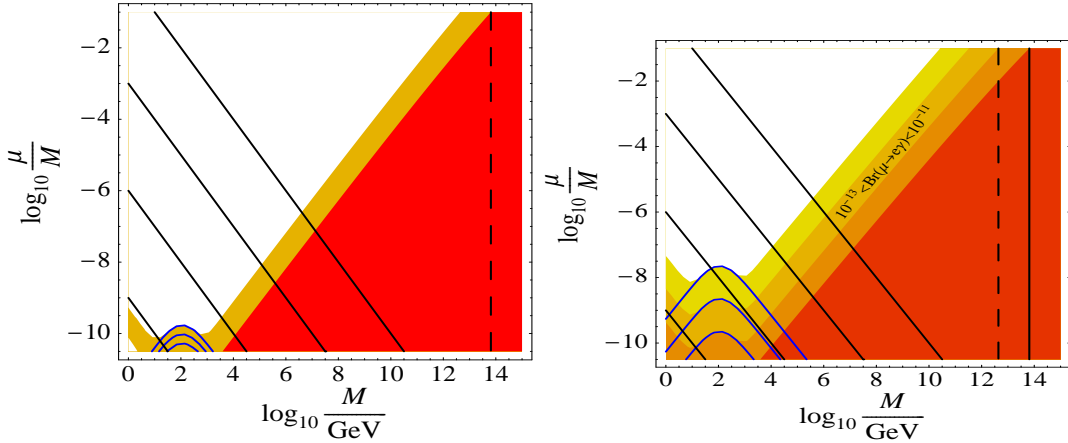


Figure 14:  $Br(\mu \rightarrow e\gamma)$  in the supersymmetric inverse seesaw model of Ref. [103].

be directly produced at accelerators [107]. Note that in order to have low  $M$  then  $\mu$  should be rather small, to keep neutrinos light. This is indicated by the diagonal lines, which indicate contours (top to bottom) of constant  $\mu = 1, 10^{-3}, 10^{-6}, 10^{-9}$  GeV. The vertical lines are contours of  $Br(\mu \rightarrow e\gamma)$  in the standard supersymmetric seesaw.

Similarly, the rates for the nuclear  $\mu^- - e^-$  conversion in Fig. 13 [108] fall within the sensitivity of future experiments such as PRISM [109].

#### 5.4.4 Reconstructing neutrino mixing at accelerators

Low-scale models of neutrino mass, considered in Sec. 3.2, offer the tantalizing possibility of reconstructing neutrino mixing at high energy accelerators, like the "Large Hadron Collider" (LHC) and the "International Linear Collider" (ILC).

A remarkable example is provided by the models where supersymmetry is the origin of neutrino mass [45], considered in Sec. 3.2.2. A general feature of these models is that, unprotected by any symmetry, the lightest supersymmetric particle (LSP) is unstable. In order to reproduce the masses indicated by current neutrino oscillation data, the LSP is expected to decay inside the detector [50] [110].

More strikingly, LSP decay properties correlate with neutrino mixing angles. For example, if the LSP is the lightest neutralino, it should have the same decay rate into muons and taus, since the observed atmospheric angle is close to  $\pi/4$  [111–113]. Similar correlations hold irrespective of which supersymmetric particle is the LSP [114] and constitute a smoking gun signature of this proposal that will be tested at upcoming accelerators.

There are other examples of low-scale models that nicely illustrate the possibility

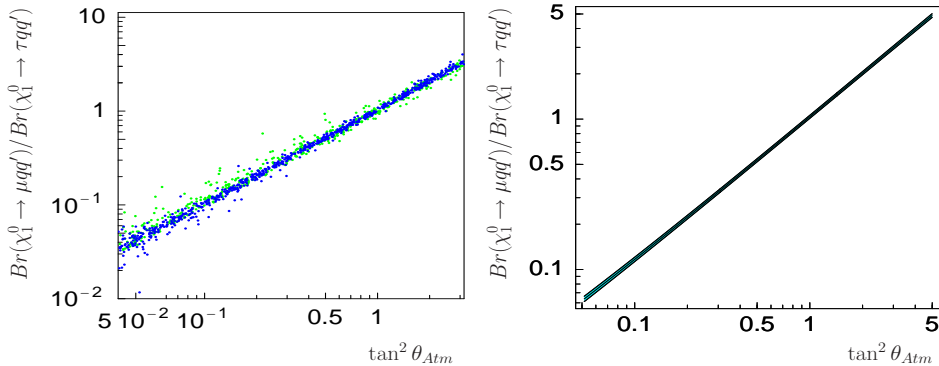


Figure 15: LSP decays trace the atmospheric mixing angle [111].

of probing neutrino properties at accelerators [115].

## 5.5 Thermal leptogenesis

Now we briefly discuss one of the cosmological implications of neutrino masses and mixing, in the context of seesaw schemes. It has long been noted [116] that seesaw models open an attractive possibility of accounting for the observed cosmological matter-antimatter asymmetry in the Universe through the leptogenesis mechanism [117]. In this picture the decays of the heavy “right-handed” neutrinos present in the seesaw play a crucial role. These take place through diagrams in Fig. 16. In order to induce successful leptogenesis the decay must happen before the electroweak phase transition [118] and must also take place out-of-equilibrium, i. e. the decay rate must be less than the Hubble expansion rate at that epoch. Another crucial ingredient is CP violation in the lepton sector. The lepton (or B-L) asymmetry thus produced then gets

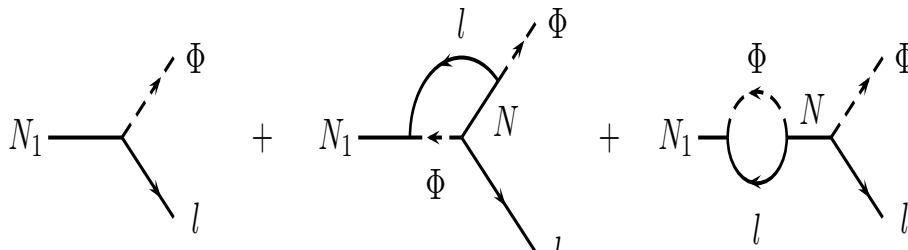


Figure 16: Diagrams contributing to leptogenesis.

converted, through sphaleron processes, into the observed baryon asymmetry.

In the framework of a supersymmetric seesaw scheme the high temperature needed for leptogenesis leads to an overproduction of gravitinos, which destroys the standard predictions of Big Bang Nucleosynthesis (BBN). In minimal supergravity models, with

$m_{3/2} \sim 100$  GeV to 10 TeV gravitinos are not stable, decaying during or after BBN. Their rate of production can be so large that subsequent gravitino decays completely change the standard BBN scenario. To prevent such “gravitino crisis” one requires an upper bound on the reheating temperature  $T_R$  after inflation, since the abundance of gravitinos is proportional to  $T_R$ . A recent detailed analysis derived a stringent upper bound  $T_R \lesssim 10^6$  GeV when the gravitino decay has hadronic modes [119].

This upper bound is in conflict with the temperature required for leptogenesis,  $T_R > 2 \times 10^9$  GeV [120]. Therefore, thermal leptogenesis seems difficult to reconcile with low energy supersymmetry if gravitino masses lie in the range suggested by the simplest minimal supergravity models. Their required mass is typically too large in order for them to be produced after inflation, implying that the minimal type I supersymmetric seesaw schemes may be in trouble. Two recent suggestions have been made to cure this inconsistency.

One proposal [121] was to add a small R-parity violating  $\lambda_i \hat{\nu}_i^c \hat{H}_u \hat{H}_d$  term in the superpotential, where  $\hat{\nu}_i^c$  are right-handed neutrino supermultiplets. One can show that in the presence of this term, the produced lepton-antilepton asymmetry can be enhanced. An alternative suggestion [122] was made in the context of the extended supersymmetric seesaw scheme considered in Sec. 3.1.5. It was shown in this case that leptogenesis can occur at the TeV scale through the decay of a new singlet, thereby avoiding the gravitino crisis. Washout of the asymmetry is effectively suppressed by the absence of direct couplings of the singlet to leptons.

## 6 Non-standard neutrino interactions

Most neutrino mass generation mechanisms imply the existence of dimension-6 sub-weak strength  $\varepsilon G_F$  non-standard neutrino interaction (NSI) operators, as illustrated in Fig. 17. These NSI can be of two types: flavour-changing (FC) and non-universal (NU). They are conceptually interesting for neutrino propagation since their presence leads to the possibility of resonant neutrino conversions even in the absence of masses [123].

NSI may arise from the non-trivial structure of charged and neutral current weak interactions characterizing seesaw-type schemes [9]. While their expected magnitude is rather model-dependent, it may well fall within the range that will be tested in future precision studies [68]. For example, in inverse seesaw model of Sec. 3.2.3 the non-unitary piece of the lepton mixing matrix can be sizeable and hence the induced non-

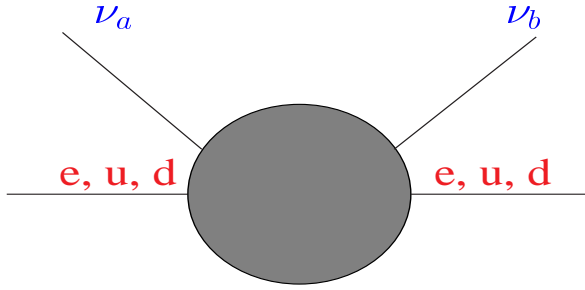


Figure 17: Flavour-changing effective operator for non-standard neutrino interaction.

standard interactions may be phenomenologically important. With neutrino physics entering the precision age it becomes a challenge to scrutinize the validity of the unitary approximation to the lepton mixing matrix, given its theoretical fragility [9].

Relatively sizable NSI strengths may also be induced in supersymmetric unified models [100] and models with radiatively induced neutrino masses, discussed in Sec. 3.2.1.

## 6.1 Atmospheric neutrinos

The Hamiltonian describing atmospheric neutrino propagation in the presence of NSI has, in addition to the usual oscillation part, another term  $H_{\text{NSI}}$ ,

$$H_{\text{NSI}} = \pm\sqrt{2}G_F N_f \begin{pmatrix} 0 & \varepsilon \\ \varepsilon & \varepsilon' \end{pmatrix}. \quad (52)$$

Here  $+$ ( $-$ ) holds for neutrinos (anti-neutrinos) and  $\varepsilon$  and  $\varepsilon'$  parameterize the NSI:  $\sqrt{2}G_F N_f \varepsilon$  is the forward scattering amplitude for the FC process  $\nu_\mu + f \rightarrow \nu_\tau + f$  and  $\sqrt{2}G_F N_f \varepsilon'$  represents the difference between  $\nu_\mu + f$  and  $\nu_\tau + f$  elastic forward scattering (NU).  $N_f$  is the number density of the fermion  $f$  along the neutrino path.

It has been shown [124] that in such 2-neutrino approximation, the determination of atmospheric neutrino parameters  $\Delta m_{\text{ATM}}^2$  and  $\sin^2 \theta_{\text{ATM}}$  is hardly affected by the presence of NSI on down-type quarks ( $f = d$ ). Future neutrino factories will substantially improve this bound [125].

## 6.2 Solar neutrinos

Are solar oscillations robust? Do we understand the Sun, neutrino propagation and neutrino interactions well enough to trust current oscillation parameter determinations? Reactors have played a crucial role in identifying oscillations as “the” solution to the solar neutrino problem [62].

Thanks to KamLAND we have ruled out an otherwise excellent solution of the solar neutrino problem based on spin-flavour precession due to convective zone magnetic fields [126, 127]. The absence of solar anti-neutrinos in KamLAND [128] has been used to establish robustness of the LMA solution with respect to spin-flavour precession due to convective zone magnetic fields.

Thanks to KamLAND one could also establish robustness of the LMA solution with respect to small density fluctuations in the solar interior [129, 130], as could arise, say, from solar radiative zone magnetic fields [131].

Finally, again thanks to KamLAND we have ruled out an otherwise excellent solution of the solar neutrino problem based on non-standard neutrino interactions [132]. However, in contrast to the atmospheric case, non-standard physics may still affect neutrino propagation properties and detection cross sections in ways that can affect current determinations [133]. This implies that the oscillation interpretation of solar neutrino data is still “fragile” with respect to the presence of non-standard interactions in the  $e - \tau$  sector, though the required NSI strength for non-robustness to set in is quite large. In contrast, one can show that even a small residual non-standard interaction of neutrinos in this channel can have dramatic consequences for the sensitivity to  $\theta_{13}$  at a neutrino factory [134]. It is therefore important to improve the sensitivities on NSI, another window of opportunity for neutrino physics in the precision age.

## Acknowledgements

I thank the organizers for hospitality at Corfu. This work was supported by a Humboldt research award at the Institut für Theoretische Physik of the Universität Tübingen, and also by Spanish grants FPA2005-01269/BFM2002-00345, European commission RTN Contract MRTN-CT-2004-503369 and ILIAS/N6 Contract RII3-CT-2004-506222. I thank T. Rashba for proof-reading.

## References

- [1] Super-Kamiokande collaboration, S. Fukuda *et al.*, Phys. Lett. **B539**, 179 (2002), [hep-ex/0205075].
- [2] SNO collaboration, Q. R. Ahmad *et al.*, Phys. Rev. Lett. **89**, 011301 (2002), [nucl-ex/0204008].
- [3] KamLAND collaboration, T. Araki *et al.*, Phys. Rev. Lett. **94**, 081801 (2004).